Complex Path Integrals and Saddles in Two-Dimensional Gauge Theory

P. V. Buividovich,[1,*] Gerald V. Dunne,[2,†] and S. N. Valgushev[1,3,‡]
[1]Institute for Theoretical Physics, Regensburg University, D-93053 Regensburg, Germany
[2]Department of Physics, University of Connecticut, Storrs, Connecticut 06269-3046, USA
[3]Institute of Theoretical and Experimental Physics (ITEP), B. Cheremushkinskaya Street 25, 117218 Moscow, Russia
(Received 15 January 2016; published 30 March 2016)

We study numerically the saddle point structure of two-dimensional lattice gauge theory, represented by the Gross-Witten-Wadia unitary matrix model. The saddle points are, in general, complex valued, even though the original integration variables and action are real. We confirm the trans-series and instanton gas structure in the weak-coupling phase, and we identify a new complex-saddle interpretation of nonperturbative effects in the strong-coupling phase. In both phases, eigenvalue tunneling refers to eigenvalues moving off the real interval, into the complex plane, and the weak-to-strong coupling phase transition is driven by saddle condensation.

DOI: 10.1103/PhysRevLett.116.132001

Introduction.—Path integral saddle points are physically important in quantum mechanics, matrix models, quantum field theory (QFT), and string theory, and they are deeply related to the typical asymptotic nature of weak-coupling perturbative expansions. Such relations are central to the concept of *resurgence*, whereby different saddles are intertwined by monodromy properties that connect them and account for Stokes phases. The theory of resurgence has recently provided new insights into matrix models and string theories [1–6], and it has been applied to asymptotically free QFTs and sigma models [7–10], and localizable supersymmetric QFTs [11]. One motivation for such QFT studies is to find a practical numerical implementation of a semiclassical expansion that could provide a Picard-Lefschetz thimble decomposition of gauge theory, either in the continuum or on the lattice, especially for theories with a sign problem [12,13]. A unifying theme in these studies, and in related work [14–17], is the appreciation that *complex* saddles are important, particularly in the context of phase transitions, even though the original "path integral" may be a sum over only real configurations.

In gauge theories, there are two physical parameters which control the strength of fluctuations around the saddle points and enter the resurgent trans-series expansion: the rank N of the gauge group and the 't Hooft coupling $\lambda \equiv Ng^2$, with gauge coupling g^2 [18]. The interplay between the dependence on N and λ leads to novel effects [1,2,6] which we explore here. An important goal would be to construct uniform resurgent approximations [19] (with respect to λ and $1/N$) which analytically relate the weak- and strong-coupling phases. For gauge theories, such a relation would certainly improve our understanding of confinement and dynamical mass gap generation. It would also extend the applicability of diagrammatic Monte Carlo studies of non-Abelian lattice gauge theories, which thus far are limited to the regime of unphysically strong bare coupling constants [20].

The difference between weak- and strong-coupling phases is particularly dramatic in the large-N limit of 2D gauge theories, where they are separated by a third-order phase transition with respect to the 't Hooft coupling λ [21–24] and/or the manifold area A [25,26]. Physically, on the weak-coupling side this large-N phase transition in 2D gauge theory is related to the condensation of instantons [24,26,27], which are exponentially suppressed at a large N away from the transition point. Much less is known about the role of instantons (or other saddles) on the strong-coupling side of this transition, except in the double-scaling limit. Here, we study the simplest example of 2D lattice gauge theory, the Gross-Witten-Wadia unitary matrix model [21–23], to demonstrate the novel properties of complex saddles in the strong-coupling phase as well as their relation to the resurgent structure of the $1/N$ expansion.

Gross-Witten-Wadia (GWW) model.—The partition function is the integral $\mathcal{Z} = \int \mathcal{D}U \exp[(N/\lambda)\mathrm{Tr}(U+U^\dagger)]$ over $N \times N$ unitary matrices $U \in U(N)$. $\mathcal{Z}$ can be expressed in terms of the eigenvalues e^{iz_i} of U [21,22]:

$$\begin{aligned}
\mathcal{Z} &= \prod_{i=1}^{N} \int_{-\pi}^{\pi} dz_i e^{-S(z_i)}, \\
S(z_i) &= \sum_i V(z_i) - \ln \Delta^2(z_i), \\
V(z) &= -\frac{2N}{\lambda}\cos(z), \\
\Delta(z_i) &= \prod_{i<j} \sin\left(\frac{z_i - z_j}{2}\right).
\end{aligned} \tag{1}$$

As $N \to \infty$, the leading contribution is from a distribution of eigenvalues z_i along the line $\mathrm{Re}z \in [-\pi,\pi)$, $\mathrm{Im}z = 0$, with a density function $\rho(z)$, such that the number of

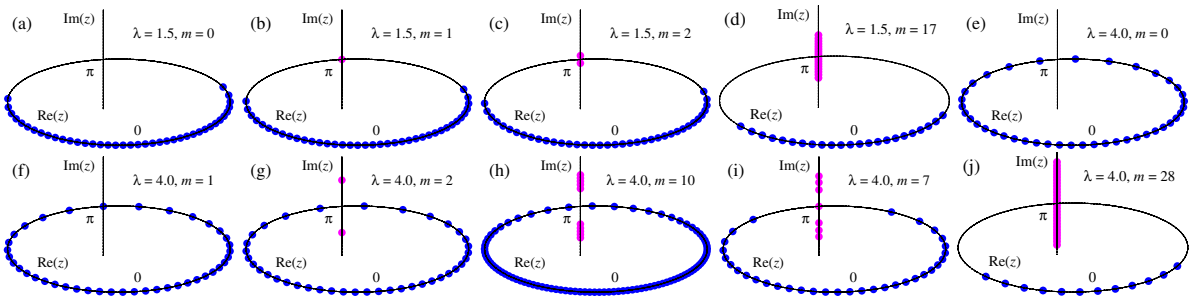

FIG. 1. Saddle point configurations of eigenvalues z_i in the (a)–(d) weak-coupling and (e)–(j) strong-coupling phases with different "instanton numbers" m. $N = 40$ on all of the plots except for (h), where we take $N = 100$ in order to illustrate the three-cut solution at a large m and strong coupling.

eigenvalues in the interval $[z, z + dz]$ is $dn = N\rho(z)dz$. Writing the action S in terms of $\rho(z)$ identifies the large parameter N^2 in the exponent of the integrand, motivating a saddle point analysis. At $N = \infty$ this model has a third-order phase transition at $\lambda_c = 2$, where the third derivative of the free energy $E_0(\lambda) = -\log \mathcal{Z}/N^2$ is discontinuous [21,22].

The GWW model is more than a toy model: it exhibits the generic phenomenon of phase transitions driven by gap closing in eigenvalue distributions [2,28], which is also accompanied by the condensation of Lee-Yang zeros in the complex coupling space [29] and which is common in numerous physical systems, such as 2D continuum gauge theory [25,26] and four-dimensional gauge theory at a large N [30], string theory [31,32], large-N Chern-Simons theory [33], general unitary and Hermitian matrix models [2,6], and applications in mesoscopic conductance [34] and entanglement entropy [35].

Complex saddles in the GWW model.—We numerically solve the saddle equations $(\partial S/\partial z_i) = 0$, $z_i \in \mathbb{C}$ at a large but finite N. We use the next-order improved Newton iterations, the Halley method [36,37]. We find complex saddles with novel properties not directly visible at $N = \infty$.

In both phases, we find saddle configurations z_i consisting of $(N - m)$ real eigenvalues located on the line $\mathrm{Re}z \in [-\pi,\pi)$, $\mathrm{Im}z = 0$, and m complex eigenvalues on the line $z = \pi + iy$, $y \in \mathbb{R}$. These lines are the steepest ascent contours of the potential $V(z)$, originating from its extrema at $z = 0$ and $z = \pi$. The saddle configurations of z_i are all symmetric with respect to these points; so, for odd m there is always one eigenvalue exactly at $z = \pi$. Examples of saddle configurations in both phases are shown in Fig. 1 for various values of m. The action for these saddles has a real part plotted in Fig. 2, as a function of m, for three different values of λ: below, at, and above the phase transition. The imaginary part of $S(z)$ is always a multiple of π: $\mathrm{Im}S(z) = \pi\lfloor m/2 \rfloor$, where $\lfloor \cdot \rfloor$ is the floor function, so that the weight $\exp[-S(z)]$ is always real but can have either sign. This sign comes exclusively from the Vandermonde determinant $\Delta^2(z)$, and it is interpreted as a hidden topological angle [38].

Vacuum saddle.—We identify the $m = 0$ saddle with the planar ($N = \infty$) contribution. As seen in Fig. 1, in the weak-coupling phase, the $m = 0$ saddle has a gapped distribution of real eigenvalues localized around the stable point $z = 0$. At the phase transition $\lambda = 2$, this distribution closes at $z = \pi$, becoming ungapped in the strong-coupling phase. As shown in Fig. 3, the numerical distribution of eigenvalues fits the $N = \infty$ forms [21,22],

$$\rho^{(w)}(z) = \frac{2}{\lambda\pi}\cos\left(\frac{z}{2}\right)\sqrt{\frac{\lambda}{2} - \sin^2\left(\frac{z}{2}\right)}, \quad \lambda < 2 \tag{2}$$

$$\rho^{(s)}(z) = \frac{1}{2\pi}\left(1 + \frac{2}{\lambda}\cos(z)\right), \quad \lambda > 2. \tag{3}$$

Thus, the numerical $m = 0$ free energy, $-S_0/N^2$, shows the expected third-order phase transition at $\lambda = 2$.

Nonvacuum saddles at weak coupling.—For $\lambda < 2$, the lowest action nonperturbative saddle has $m = 1$, with one eigenvalue at $z = \pi$, and has a real action (relative to the vacuum action) exactly matching the weak-coupling instanton action $S_I^{(w)}$ [2] (see Fig. 4),

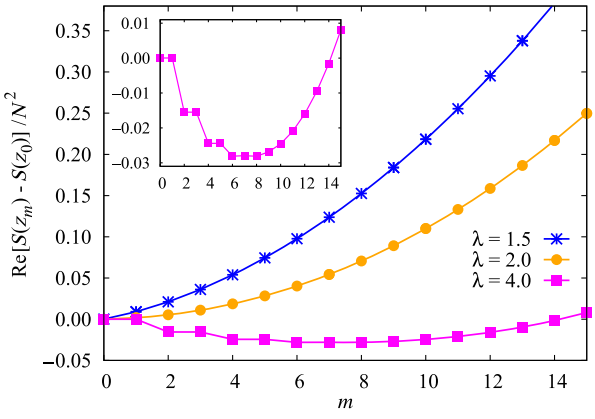

FIG. 2. Real part of the saddle action, $\mathrm{Re}S(z)$, versus the instanton number m, for different values of λ, at $N = 40$. (Inset) $\mathrm{Re}S(z)$ vs m at $\lambda = 4$ on a larger scale.

$$S_I^{(w)} = 4/\lambda\sqrt{1-\lambda/2} - arccosh[(4-\lambda)/\lambda], \qquad \lambda < 2. \tag{4}$$

As m increases, m eigenvalues line up along the imaginary direction $z = \pi + iy$, forming a cut (see Fig. 1). This is a numerical indication of "eigenvalue tunneling," but we note that the tunneled eigenvalues are complex. For a small $m \ll N$, we find the conventional picture of a dilute instanton gas, with the real part of the action lowest at $m = 0$, and scaling approximately linearly with m, as $\mathrm{Re}(S_m - S_0) = mNS_I^{(w)}$ for $m \ll N$, with $S_I^{(w)}$ being the weak-coupling instanton action (4). We thus identify the integer m, the number of eigenvalues along the imaginary direction, with the instanton number in the weak-coupling phase. The m-instanton saddles have Hessian fluctuation matrices, $H_{m,ij} = (\partial^2 S_m/\partial z_i \partial z_j)$, with m negative modes (see Fig. 5). Thus, the $m = 1$ saddle gives an imaginary contribution to the saddle expansion of the free energy; we have confirmed that this is canceled by an imaginary term from the Borel summation of the divergent fluctuations about the $m = 0$ vacuum saddle, a clear indication of resurgent cancellations. This can be traced to the resurgent asymptotics of individual Bessel functions, using the determinant representation [21,22] of the partition function: $\mathcal{Z} = \det[(I_{j-k}(2N/\lambda)]$.

Saddle condensation phase transition.—As $\lambda \to 2$ from the weak-coupling side, the gap in the real part of the eigenvalue distribution closes at the unstable point ($z = \pi$) (see Figs. 1 and 3). Furthermore, as seen in Fig. 2, the real part of the saddle action, relative to the vacuum value, tends to zero, so that all instantons with $m \ll N$ become equally important at the transition point, signaling instanton condensation [2,24,26].

Nonvacuum saddles at strong coupling.—Since the unstable point $z = \pi$ is already in the support of $\rho^{(s)}(z)$, in the conventional picture nonvacuum saddles can no longer be constructed by dragging eigenvalues to $z = \pi$. Nevertheless, Mariño obtained the following strong-coupling "instanton action" using a trans-series ansatz in the string equation [2] (see also Appendix B in Ref. [39]):

$$S_I^{(s)} = 2arccosh(\lambda/2) - 2\sqrt{1-4/\lambda^2}, \qquad \lambda \geq 2. \tag{5}$$

Our numerical approach yields a natural interpretation of this "instanton" as a saddle configuration, with complex eigenvalue tunneling from the real to the imaginary axis (see Fig. 1). As in the weak-coupling phase, m eigenvalues line up along the imaginary direction, but these strong-coupling saddles have some surprising properties.

(i) In the strong-coupling phase, at a large N, the $m = 1$ saddle has real action degenerate with that of the $m = 0$ saddle, up to exponentially small corrections precisely of the form $\exp(-N/2S_I^{(s)})$, where $S_I^{(s)}(\lambda)$ is the strong-coupling instanton action (5); see Fig. 6. Physically, this is due to a quasizero mode in the strong-coupling regime. The $m = 0$ and $m = 1$ configurations have the same continuous eigenvalue density but differ microscopically by the presence or absence of a single eigenvalue at $z = \pi$ [see Figs. 1(e) and 1(f)]. To leading order in $1/N$, they can be related by a shift of every eigenvalue to the middle of the interval to its neighboring eigenvalue. At a large N this interval is inversely proportional to the density function $\rho(z)$, so the shift of all eigenvalues by $\delta z_i \sim 1/\rho(z_i)$ is a flat direction of the action. Correspondingly, at $N \to \infty$, δz_i is the eigenvector of the Hessian $H_{ij} = (\partial^2 S/\partial z_i \partial z_j)$ with zero eigenvalue [40]. Numerically, we have found that as $N \to \infty$, the lowest eigenvalue ξ_0 vanishes exponentially fast as $\exp(-N/2S_I^{(s)})$ (see Figs. 5 and 6). Interestingly, this is the same exponential factor seen in the splitting $\mathrm{Re}(S_1 - S_0)$.

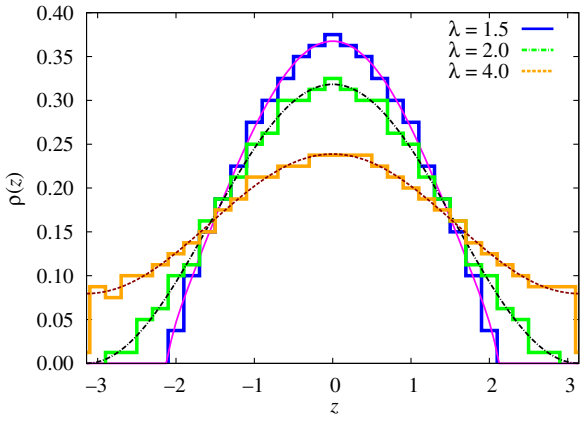

FIG. 3. Numerical eigenvalue distributions for the $m = 0$ saddle [$N = 400$], compared with the analytic $\rho(z)$ in Eqs. (2) and (3).

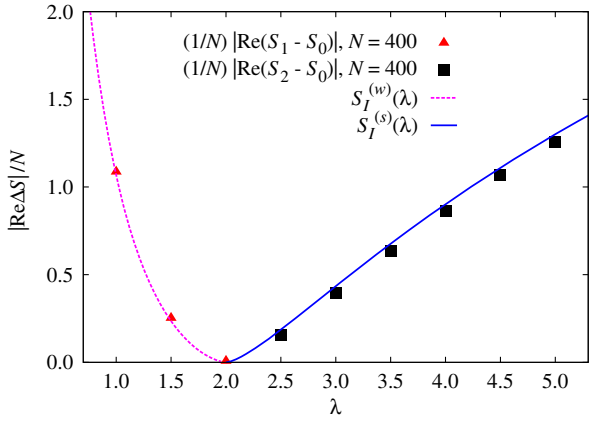

FIG. 4. Numerical results (dots) for the relative actions of the leading nonvacuum saddles with $m = 1$ (in the weak-coupling phase) and $m = 2$ (in the strong-coupling phase) at $N = 400$. Solid lines are the analytic expressions (4) and (5).

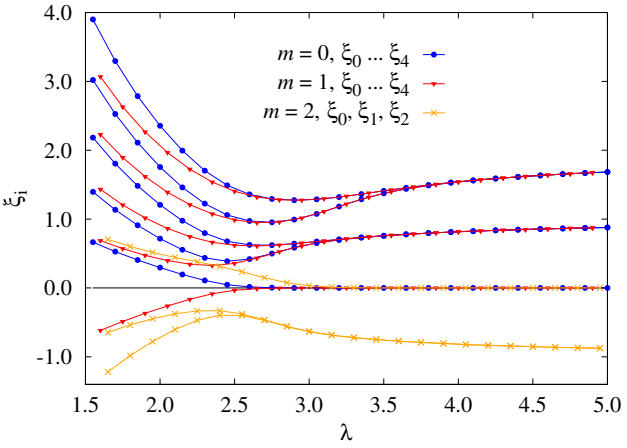

FIG. 5. Several of the lowest eigenvalues ξ_i of the Hessian matrix $H_{m,ij} = (\partial^2 S_m/\partial z_i \partial z_j)$ for saddles with $m = 0$, 1, 2 at $N = 40$. There are m negative modes, and at strong coupling all modes, except the quasizero mode, become quasidegenerate.

(ii) At strong coupling, it is not the $m = 1$ saddle, but rather the $m = 2$ saddle which we identify as the "strong-coupling instanton" configuration. This saddle is manifestly complex [Fig. 1(g)]. It has an action with a real part equal to, as a function of λ, the modulus of the strong-coupling action (5): $|\mathrm{Re}(S_2 - S_0)| = NS_I^{(s)}(\lambda)$, as shown in Fig. 4. This reversal of sign is a numerical example of a phenomenon found in the context of the Painlevé equations, where formal trans-series arise with saddles of both signs of the action [4,5,41].

(iii) At strong coupling, as m increases more eigenvalues move away from the real axis, forming a distinct two-cut structure around $z = \pi$ (with one eigenvalue in the gap at $z = \pi$ if m is odd); see Fig. 1(h). The real part of the action decreases with m until it reaches a critical value $m^\star$, after

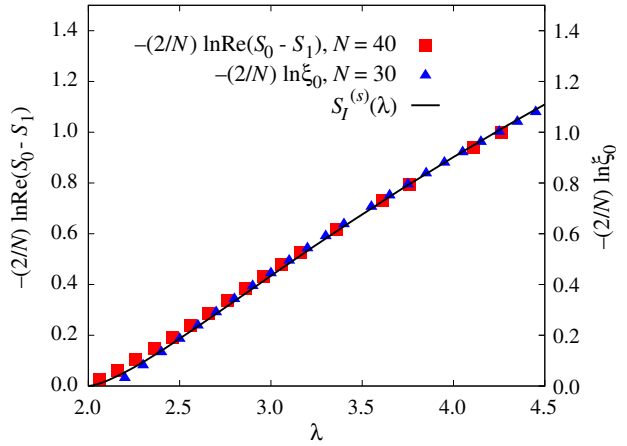

FIG. 6. Comparison of the log of the difference between the actions of the $m = 0$ and $m = 1$ saddles (left vertical axis), and the log of the lowest Hessian eigenvalue ξ_0 (right vertical axis), in the strong-coupling phase, with half of the strong-coupling instanton action in Eq. (5). Both effects are governed by the same exponential.

which it increases again; see Fig. 2. When m reaches $m^\star$ the gap between the two cuts closes, and at the same time the distribution of the remaining eigenvalues on the real axis becomes gapped [Figs. 1(i) and 1(j)]. The saddle point action scales linearly with m for $m \ll m^\star$: $|\mathrm{Re}(S_m - S_0)| \approx \lfloor m/2 \rfloor NS_I^{(s)}$, where $S_I^{(s)}$ is the strong-coupling instanton action (5). Note the floor function in this expression, which implies that the aforementioned degeneracy of the action for $m = 0$ and $m = 1$ persists also for the pairs of saddle points with $m = 2n$ and $m = 2n + 1$, for $m < m^\star$ (see the "stairs" at low m in the inset in Fig. 2). Correspondingly, the Hessian matrices for all saddles with $m < m^\star$ have quasizero modes, vanishing exponentially with N (see Fig. 5), as for the $m = 1$ saddle, but with an m-dependent prefactor.

(iv) As in the weak-coupling phase, at strong coupling the Hessian matrix for the m saddle has m negative modes (see Fig. 5). However, in the strong-coupling phase, all eigenvalues except for the zero mode become doubly degenerate, with degeneracy splitting governed again by the exponentially small quantity $\exp(-N/2S_I^{(s)}(\lambda))$.

Our numerical results indicate that the GWW partition function and free energy also have trans-series expansions in the strong-coupling phase due to complex saddle points. This provides a (complex) saddle interpretation of Mariño's trans-series result from the string equation [2] and is also consistent with the double-scaling limit described by the McLeod-Hastings solution to the Painlevé II equation, valid near the phase transition. On the weak-coupling side this solution has exponential corrections $\sim \exp(-NS_I^{(w)})$, while on the strong-coupling side the leading behavior is already exponential $\exp(-N/2S_I^{(s)})$, which implies $\exp(-NS_I^{(s)})$ behavior for the free energy [2]. Furthermore, deep in the strong-coupling region, with $\lambda \gg 2$, and using the method of orthogonal polynomials, Goldschmidt found [39] corrections behaving like $(1/N^2)(\lambda/e)^{-2N} \sim (1/N^2)\exp[-NS_I^{(s)}(\lambda)]$ [note that $S_I^{(s)} \sim 2\ln(\lambda/e) + (2/\lambda^2) + \ldots$, for $\lambda \gg 2$].

Conclusions.—Our numerical study reveals a surprisingly rich structure of complex-valued saddles in both the weak- and strong-coupling phases of two-dimensional lattice gauge theory, represented by the Gross-Witten-Wadia unitary matrix model. These complex saddles are intimately related to the resurgent structure of the $1/N$ expansion. We find a new complex-saddle interpretation of Mariño's strong-coupling instanton action, and these saddles have novel physical properties. There is clear numerical evidence for instanton condensation at the transition. In both phases, eigenvalue tunneling produces complex saddles, and these results suggest a Lefschetz thimble interpretation of the saddle point expansion. Given the direct relation between the instanton actions in the matrix model (1) and in 2D continuum gauge theory [2], we expect similar results for complex-valued saddles to apply also to continuum 2D gauge theories [25,26].

We thank T. Sulejmanpasic and M. Ünsal for the interesting and stimulating discussions. This work was supported by the S. Kowalevskaja Award from the Alexander von Humboldt Foundation (P. B. and S. V.), and by U.S. DOE Grant No. DE-SC0010339 (G. D.).

*pavel.buividovich@physik.uni-regensburg.de
†dunne@phys.uconn.edu
‡semen.valgushev@physik.uni-regensburg.de

[1] M. Mariño, R. Schiappa, and M. Weiss, Commun. Num. Theory Phys. **2**, 349 (2008).
[2] M. Mariño, J. High Energy Phys. 12 (2008) 114.
[3] S. Pasquetti and R. Schiappa, Ann. Henri Poincaré **11**, 351 (2010).
[4] S. Garoufalidis, A. Its, A. Kapaev, and M. Marino, Int. Math. Res. Not. **2012**, 561 (2012).
[5] I. Aniceto, R. Schiappa, and M. Vonk, Commun. Num. Theory Phys. **6**, 339 (2012).
[6] R. Couso-Santamaría, R. Schiappa, and R. Vaz, Ann. Phys. (Berlin) **356**, 1 (2015).
[7] P. C. Argyres and M. Unsal, J. High Energy Phys. 08 (2012) 063.
[8] G. V. Dunne and M. Unsal, J. High Energy Phys. 11 (2012) 170.
[9] A. Cherman, D. Dorigoni, G. V. Dunne, and M. Unsal, Phys. Rev. Lett. **112**, 021601 (2014).
[10] G. V. Dunne and M. Unsal, J. High Energy Phys. 09 (2015) 199.
[11] I. Aniceto, J. G. Russo, and R. Schiappa, J. High Energy Phys. 03 (2015) 172.
[12] M. Cristoforetti, F. Di Renzo, and L. Scorzato, Phys. Rev. D **86**, 074506 (2012).
[13] H. Fujii, D. Honda, M. Kato, Y. Kikukawa, S. Komatsu, and T. Sano, J. High Energy Phys. 10 (2013) 147.
[14] F. David, Phys. Lett. B **302**, 403 (1993).
[15] E. Witten, in *Chern-Simons Gauge Theory: 20 Years After*, edited by J. E. Andersen, H. U. Boden, A. Hahn, and B. Himpel, AMS/IP Studies in Advanced Mathematics Vol. 50 (American Mathematical Society, Providence, 2011), p. 347.
[16] D. Harlow, J. Maltz, and E. Witten, J. High Energy Phys. 12 (2011) 071.
[17] C. K. Dumlu and G. V. Dunne, Phys. Rev. D **84**, 125023 (2011).
[18] M. Marino, *Instantons and Large N: An Introduction to Non-Perturbative Methods in Quantum Field Theory* (Cambridge University Press, Cambridge, England, 2015).
[19] G. Basar and G. V. Dunne, J. High Energy Phys. 02 (2015) 160.
[20] P. de Forcrand, J. Langelage, O. Philipsen, and W. Unger, Phys. Rev. Lett. **113**, 152002 (2014).
[21] D. J. Gross and E. Witten, Phys. Rev. D **21**, 446 (1980).
[22] S. R. Wadia, arXiv:1212.2906.
[23] S. R. Wadia, Phys. Lett. **93B**, 403 (1980).
[24] H. Neuberger, Nucl. Phys. **B179**, 253 (1981).
[25] M. R. Douglas and V. A. Kazakov, Phys. Lett. B **319**, 219 (1993).
[26] D. J. Gross and A. Matytsin, Nucl. Phys. **B429**, 50 (1994).
[27] H. Neuberger, Phys. Lett. **94B**, 199 (1980).
[28] S. N. Majumdar and G. Schehr, J. Stat. Mech. (2014) P01012.
[29] K. S. Kölbig and W. Rühl, Z. Phys. C **12**, 135 (1982).
[30] R. Narayanan and H. Neuberger, J. High Energy Phys. 03 (2006) 064.
[31] V. Periwal and D. Shevitz, Phys. Rev. Lett. **64**, 1326 (1990).
[32] D. J. Gross and W. Taylor, Nucl. Phys. **B400**, 181 (1993).
[33] S. Jain, S. Minwalla, T. Sharma, T. Takimi, S. R. Wadia, and S. Yokoyama, J. High Energy Phys. 09 (2013) 009.
[34] P. Vivo, S. N. Majumdar, and O. Bohigas, Phys. Rev. Lett. **101**, 216809 (2008).
[35] C. Nadal, S. N. Majumdar, and M. Vergassola, Phys. Rev. Lett. **104**, 110501 (2010).
[36] E. W. Weisstein, http://mathworld.wolfram.com/HalleysMethod.html.
[37] See Supplemental Material at http://link.aps.org/supplemental/10.1103/PhysRevLett.116.132001 for a detailed description of this method.
[38] A. Behtash, T. Sulejmanpasic, T. Schäfer, and M. Ünsal, Phys. Rev. Lett. **115**, 041601 (2015).
[39] Y. Goldschmidt, J. Math. Phys. (N.Y.) **21**, 1842 (1980).
[40] See Supplemental Material at http://link.aps.org/supplemental/10.1103/PhysRevLett.116.132001 for an explicit proof.
[41] I. Aniceto and R. Schiappa, Commun. Math. Phys. **335**, 183 (2015).